A method for predicting earthquakes in advance

Xia Cao *

School of Chemistry and Biological Engineering, University of Science and Technology Beijing, Beijing, 100083, China

Beijing Institute of Nanoenergy and Nanosystems, Chinese Academy of Sciences, Beijing, 101400, China

*Corresponding Author: E-mail: caoxia@ustb.edu.cn

Abstract

The internal collision movement of the earth in the early stage of geological disasters will be different from the ordinary, and the generated signals are also unusual. The possibility of geological disasters such as earthquakes can be monitored and predicted by utilizing the changes caused by the continuous collision movement deep inside the earth. This new system based on the Collision Electro-Magnetic Theory was first proposed for monitoring geological disasters such as earthquakes, tsunamis, avalanches, volcanic eruptions, landslides, and debris flows. The system mainly consists of a collision-based power generator and a receiver. The collision-based power generator can be made from a single material or a composite of several materials. The receiver can be composed of one or more types of semiconductors, conductors, or composite materials that are resistant to high temperatures and have excellent mechanical properties. It is simple and effective, and can greatly improve the accuracy and timeliness of disaster warnings. Recognizing precursors to longitudinal waves is crucial for predicting earthquakes and minimizing both human and economic losses, and seismometers that are exempt from regular power source replacement and performance degradation under humid conditions are highly anticipated. This work draws inspiration from the three-dimensional microstructure of the superhydrophobic lotus leaf surface and transfers the microstructure from nano-SiO_2 to Ecoflex surface. A self-powered, low-cost, highly durable, and stable triboelectric nanogenerator (TENG) was thus developed for earthquake warning based on the

superhydrophobic, self-cleaning, and flame retardant film. The as-prepared TENG can convert the tiny vibration in the earth into electricity with a peak power density of 15.4 mW/m². In addition, there is a strong linear correlation (The R^2 value is 0.98 and 0.99.) between peak current and vibration acceleration and vibration when the EW-TENG is applied to different vibration intensities. It is possible to analyze the peak current to calculate the vibration intensity. Then, the real-time monitoring capability of the EW-TENG is verified in a more realistic simulated geological disaster scenario. Considering the self-power feature, it may contribute to fast earthquake response and rescue efforts, as well as research in reducing the risk of seismic hazards.

Key Words

triboelectric nanogenerator; sensor; superhydrophobicity; earthquake warning

1 Introduction

Earthquakes are short-term geological events that occur in the Earth's crust, potentially leading to a series of disasters. Intense earthquakes pose damage or collapse of buildings, bridges, and other infrastructure, threating people's lives and even triggering natural disasters such as landslides and tsunamis[1]. The detection of seismic waves shortly after an earthquake occurs and the immediate issuance of warning information to areas most likely to experience strong earthquakes is referred to as earthquake warning (EW)[2]. Seismic waves are categorized into three types based on propagation patterns: transverse waves, longitudinal waves, and surface waves, all of which propagate through the Earth's crust[3]. Longitudinal waves propagate at a fast speed, causing vertical ground motion with relatively weak destructive force, and transverse waves propagate at a slow speed with relatively strong destructive force[4]. Surface waves are hybrid waves that result from the interaction of transverse and longitudinal waves at the earth's surface. There is a popular belief that utilizing EW devices to detect longitudinal waves with fast propagation and less

destructive may be more promising[5-6]. Currently, EW devices for studying seismic activity are insufficient due to their high cost and the fact that these sensors all require periodic replacement of their power supplies, where the latter issue significantly limits their lifespan and range of applicability[7]. In addition, another major challenge for EW devices is their susceptibility to external environmental influences and damages, such as corrosion, humidity, and temperature variations.

Recently, triboelectric nanogenerators (TENGs) have gained significant attention due to their ability to harvest energy from ambient sources including vibrations, wind, water energy, and tidal energy[8–11]. Owing to their unique working mechanism, TENGs show innate superiority in scalability, wide material options, low cost, and high efficiency in low-frequency energy harvesting. Besides, the decipherable electric signal makes them perfect candidates for highly durable and stable sensors[12–15]. These TENG-based sensing devices effectively convert mechanical energy into electrical signals via displacement currents as the driving force[16], and have been proposed for continuous monitoring of various environmental stimuli in numerous areas[17]. In a study conducted by Cheng et al.[18], a carbon modified and integrated with the TENG, was applied to detect the lactate concentration in human perspiration, where the generated electricity was sufficient for the real-time detection. Hou et al.[19] utilized T-shaped TENG, a self-charging power underwater force sensor, to detect normal and tangential forces. Liu et al.[20] presented a contact-separation direct current TENG capable of harvesting low-frequency human activities, thus allowing TENG to be applied directly toward the self-powered wireless monitoring of body movements. However, there have been relatively few studies on TENG-based self-powered sensors which can be utilized for earthquake detection. Considering the low cost, long-life and self-power feature, as well as the sensitive response to low-frequency vibration, it is possible to create real-time seismic monitoring systems using the TENG-based sensor networks.

The possibility of geological disasters such as earthquakes can be monitored and

predicted by utilizing the changes caused by the continuous collision movement deep inside the earth. This new system based on the Collision Electro-Magnetic Theory was first proposed for monitoring geological disasters such as earthquakes, tsunamis, avalanches, volcanic eruptions, landslides, and debris flows. The system primarily comprises a collision-based power generator and a receiver. The power generator, relying on collisions, can be crafted from a single material or a blend of multiple materials. Meanwhile, the receiver can incorporate one or more types of semiconductors, conductors, or composite materials that are notably resilient to high temperatures and possess remarkable mechanical characteristics. Up to now, bionic functional surface has become a research hotspot in the field of TENGs[21]. Due to the distinctive advantage of a wide selection of materials, mimicking the crosslinking nature of surface structure of the lotus leaf on TENGs may also be feasible for excellent properties such as self-cleaning, corrosion resistance, and anti-fouling[22–24]. In this case, both the pronounced micro-texture and the special hydrophobic properties of the lotus leaf surface can be transferred to the surface of TENGs to form a dense layer of protective film that provides excellent protection for their sustainable operation in a humid environment[25-26].

For this end, SiO_2-Ecoflex films were modified to mimic the lotus effect. A single-electrode mode TENG was then developed on the composite film. With a large water contact angle of 152°, the film exhibits excellent superhydrophobicity, flame retardancy, and self-cleaning properties, thus promoting high durability and stability of the as-fabricated TENG in detecting the seismic waves. Moreover, the EW-TENG has been demonstrated to not only detect seismic longitudinal waves, but also charge capacitors for powering itself and other electronic devices, thus working in a self-power mode. Considering these grounds, it may help to build a low-cost and sensitive earthquake warning network that may work with high durability, and stability, thus reducing the damage caused by earthquakes.

2 Results and discussions

The possibility of geological disasters such as earthquakes can be monitored and predicted by utilizing the changes caused by the continuous collision movement deep inside the earth. This new method based on the Collision Electro-Magnetic Theory is suitable for monitoring geological disasters such as earthquakes, tsunamis, avalanches, volcanic eruptions, landslides, and debris flows. The system mainly consists of a collision-based power generator and a receiver. The collision-based power generator can be made from a single material or a composite of several materials. The receiver can be composed of one or more types of semiconductors, conductors, or composite materials that are resistant to high temperatures and have excellent mechanical properties. It is simple and effective, and can greatly improve the accuracy and timeliness of disaster warnings. Fig. 1a illustrates the preparation process of the modified Ecoflex film. Fig. 1b shows the obvious micro-texture characteristics of lotus leaf, where the waxy substances make the surface of the lotus leaf hydrophobic. The schematic preparation process of the superhydrophobic surface is shown in Fig. 1c. Figs. 1d-e shows the grid-like channels and a laser scanning pitch (λ_1=λ_2=244 μm) on the surface of the pre-treat Ecoflex film. This 3D micropatterned surface is inspired by both the surface morphology and the chemical coating of the microstructured lotus leaf[27-28]. The water contact angle of Ecoflex increased from 105 to 118° after pretreatment (Figs. 1h and S1). After coated by a composite layer with a thickness of 90 μm (Figs. 1f-g, Fig. S2), the water contact angle increases to 152° (Fig. 1i). This superhydrophobicity of the as-modified Ecofelx surface can be ascribed to its complex surface texture and the formation of intermolecular Si-Si bonds between silicone oligomer and SiO_2, as shown in Fig. S3. The single-electrode mode earthquake warning TENG (EW-TENG) constructed with the as-fabricated SiO_2-Ecoflex film as the friction layer is shown in Fig. 1j. When an earthquake occurs, the EW-TENG can determine the epicenter and amplitude of vibration by comparing the time deviation of the EW-TENG output voltage and the magnitude of the output voltage.

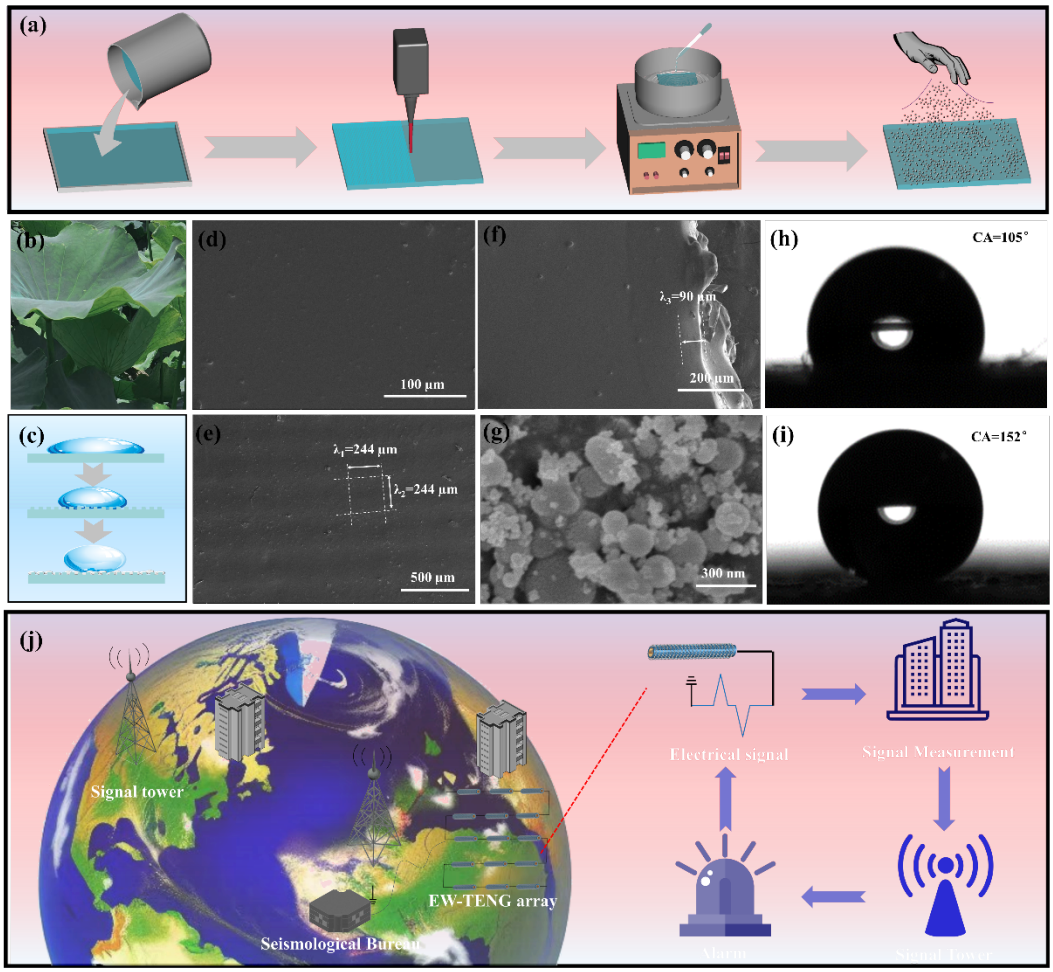

Fig. 1. Schematics of preparation process of modified Ecoflex (a). Image of the natural lotus leaf (b). Schematics of preparation process of superhydrophobic surface (c). SEM images of Ecoflex film(d), pre-treat Ecoflex film(e), Lateral modified Ecoflex film(f), and SiO_2 (g). The optical image of a water contact angle of Ecoflex (h) and modified Ecoflex (i). Schematic illustration showing the EW-TENG working as seismic wave detector for better earthquake early warning (j).

Figs. 2a and b validate the superhydrophobic property of the modified Ecoflex film, where the outlines of water, saline and milk are nearly spherical on the modified Ecoflex. Figs. 2c and d further validate the self-cleaning property of the proposed superhydrophobic film. In this test, $CuSO_4$ particles, which are utilized as contaminants to diffuse into the

film can be quickly swept away when washed by water droplets. In the fire retardancy test, (Figs. 2e, f, and Fig. S4a), the modified Ecoflex film is difficult to be ignited even exposed to the flame of an alcohol lamp for 40 s. The flame extinguishes on its own after removing the source of ignition, and the structure of the samples remains almost unchanged (Fig. S4b).

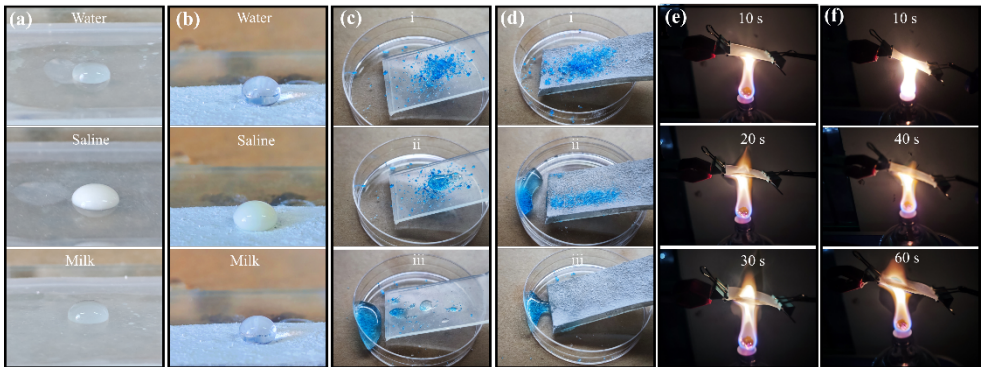

Fig. 2. Digital images of water, saline, and milk droplets on the surface of Ecoflex (a) and modified Ecoflex (b), respectively. Digital images of the self-cleaning properties of Ecoflex (c) and modified Ecoflex (d) under CuSO4 particles. Digital images of combustion tests of Ecoflex (e) and modified Ecoflex (f).

A tubular EW-TENG (100 mm in length and 10 mm in diameter) is assembled with the modified Ecoflex film as the friction layer. Fig. 3a shows the working principle of the EW-TENG, which can be explained by the coupling effects of contact electrification and electrostatic induction that are derived from the Maxwell displacement current[29–32]. Initially, when under stress from an external force, the friction layer is in full contact with the electrode. Due to the triboelectric effect, static charges transfer from the surface of the friction layer to the electrode until saturation (state i). Once the stress is released, the separation between the electrode and friction layer causes a decrease in positive charges on the electrode, requiring electrons to flow from the ground to the electrode (state ii), until an equilibrium state is reached (state iii). When stress is applied again, electrons flow from the electrode to the ground (state iv). The voltage and current signals corresponding to the

different states of the EW-TENG are shown in Fig. 2 b. The EW-TENG generates distinctive electric signals in response to various compression, either longitudinal (Fig. 3c i) or bending or lateral (Fig. 3c ii), helping the EW-TENG detect the subtle vibrations underground. The stability of the EW-TENG in complex deformation is also critical to ensure that proper function is retained during earthquakes. Fig. 3d shows that EW-TENG exhibits sufficient flexibility and toughness without any damage under the action of repeated curling, pressing, bending and other external forces.

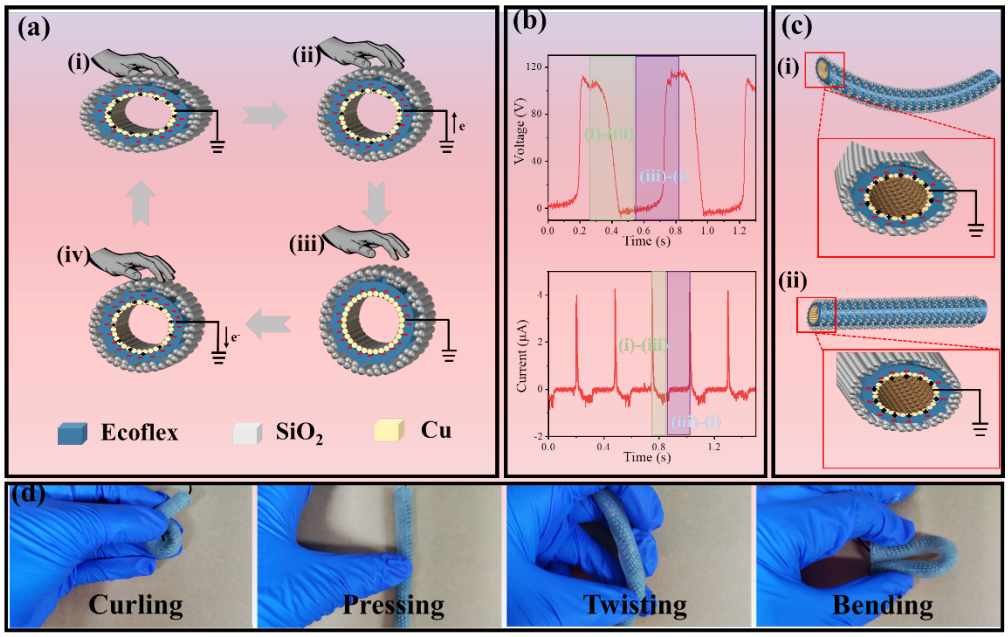

Fig. 3. Schematic diagrams of the working mechanism of EW-TENG (a). Generation of voltage and current electrical signals with respect to the different states process (b). Two different operating modes of EW-TENG including bending and squeezing (c). Digital images of the EW-TENG during curling, pressing, twisting, and bending (d).

When an earthquake occurs, the mechanical frequencies and stress directions applied to the EW-TENG are irregular, so it is necessary to investigate the output performance of the EW-TENG at different frequencies and stress directions. Figs. 4a and b show the output current and voltage of EW-TENG under stress at different directions. The inset of Fig. 4a illustrates the schematic diagram of the EW-TENG exposed to forces with different

directions. The EW-TENG outputs current and voltage under stress in different directions, including horizontal and vertical vibration directions. The output voltages of EW-TENG with bending angles of 30, 60, 90, 120, 150 and 180 degrees are tested, as shown in Fig. 4c. The output voltages proliferate from 50.2 V to 119.9 V with bending angles from 30 to 180 degrees, which are attributed to the enlarged contact area between the friction layer and the electrode with the increasing bending angle. Figs. 4d and e demonstrate the output current and voltage of the EW-TENG at different frequencies from 1 to 5 Hz. As shown, the output current of the EW-TENG increases with the frequency, and current of 7.1 μA at the frequency of 5 Hz. This significant increase correlates to the same charge in a shorter transfer time that triggers a proportional increase in the short circuit current[33-34]. The output voltage of the EW-TENG at different frequencies is about 142 V, showing no significant difference, which is due to the constant total charge of the external circuits. To measure the sensitivity of the EW-TENG, the effects of change in applied force on the output performance are investigated (Fig. 4f and g). As the force escalates from 1 N to 20 N, the output currents increase from 0.3 to 2.9 μA and the output voltages increase from 28.6 to 128.0 V. Fig. 4h illustrates the fitting line graph of voltages against stress. The pressure sensitivity (S) can be described as[35]:

$$S = \frac{\Delta V}{V_{max} \bullet \Delta P}$$

where ΔV represents the change of output voltage, V_{max} represents the maximum output voltage, and ΔP represents the change of pressure. When the EW-TENG contacts with different materials, it produces different electrical signal. By detecting this electrical signal, various materials can be identified. To demonstrate this application, six different materials, including PC, Kapton, Al, Acrylic, PTFE, and FEP, are tested with the EW-TENG, and the open circuit voltage and short circuit current are shown in Fig. 4i and j, respectively. Fig. 4k displays the output voltage of the EW-TENG under different humidity. The output voltage is maintained between 120-140 V under the relative humidities of 20%, 30%, 40%, 50%, 60% and 70%, indicating the excellent water resistance of the EW-TENG.

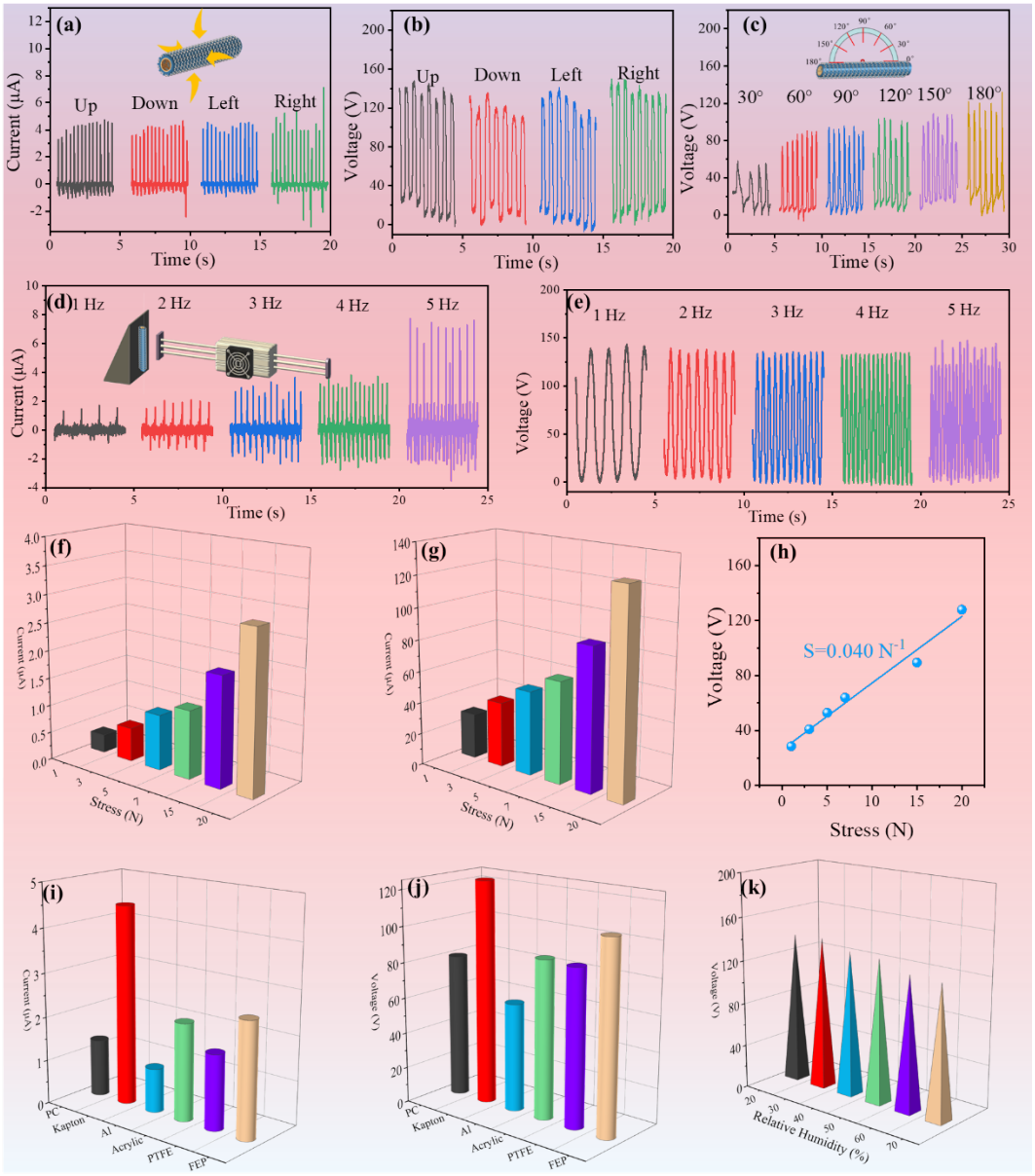

Fig. 4. Output performance of EW-TENG. Output current (a) and voltage (b) of EW-TENG subjected to stresses in different directions. Output voltage of EW-TENG at different bending states (c). Output current (d) and voltage (e) of EW-TENG at different frequencies from 1 to 5 Hz. Output current (f) and voltages (g) of EW-TENG at different forces and the fitting line graph of voltages with stress (h). Output current (i) and voltages (j) of EW-TENG with different materials. Output voltages (k) of EW-TENG at different relative humidity.

To test the stability of TENG, a durability test is conducted, as shown in Fig. 5 a. The EW-TENG exhibits an almost constant response after 5000 cycles, proving its high durability. Additionally, The EW-TENG can harvest mechanical energy and convert it into electricity to store or power electronic devices. At a frequency of 4 Hz, the output voltages and currents of the EW-TENG are tested with different load resistors, enabling the calculation of peak power and peak power density (Fig. 5b and c). In Fig. 5b, it's evident that as the load increases, the current gradually decreases while the voltage gradually increases. Fig. 5c illustrates the relationship between power density and external load. At the optimal load of 90 MΩ, the peak power reaches 0.29 mW, and the peak power density reaches 15.4 mW/m². Fig. 5d shows the voltage distribution when the EW-TENG charges a 33 μF capacitor, powering a commercial electronic watch (The inset of Fig. 5d illustrates the schematic of circuit diagram.). Initially, the EW-TENG charges a 33 μF capacitor for 80 seconds at a constant frequency of 4 Hz, in which the capacitor's voltage increases from 0 V to 4.9 V. Subsequently, the capacitor successfully powers a commercial electronic watch for 30 seconds until the capacitor's voltage drops to 1.6 V and the watch was turned off at the same time (Fig. 5e). Similarly, the EW-TENG can also power a commercial calculator (Fig. 5f). Furthermore, by directly connecting the EW-TENG to a series of LEDs, tapping the EW-TENG with the palm can illuminate up to 144 LEDs (Fig. 5g and Video S1). Fig. 5h illustrates the experimental setup of the EW-TENG for vibration response test. By comparing the peak current of EW-TENG under different seismic velocities (Fig. 5i) and seismic acceleration (Fig. 5j), the R^2 values obtained by linear fitting analysis are all above 0.98, indicating that there is a very strong linear correlation between the peak current and the vibrometer data. Consequently, the vibration acceleration and vibration velocity experienced by the EW-TENG can be calculated by analyzing the peak current, showing potential as a seismic sensor.

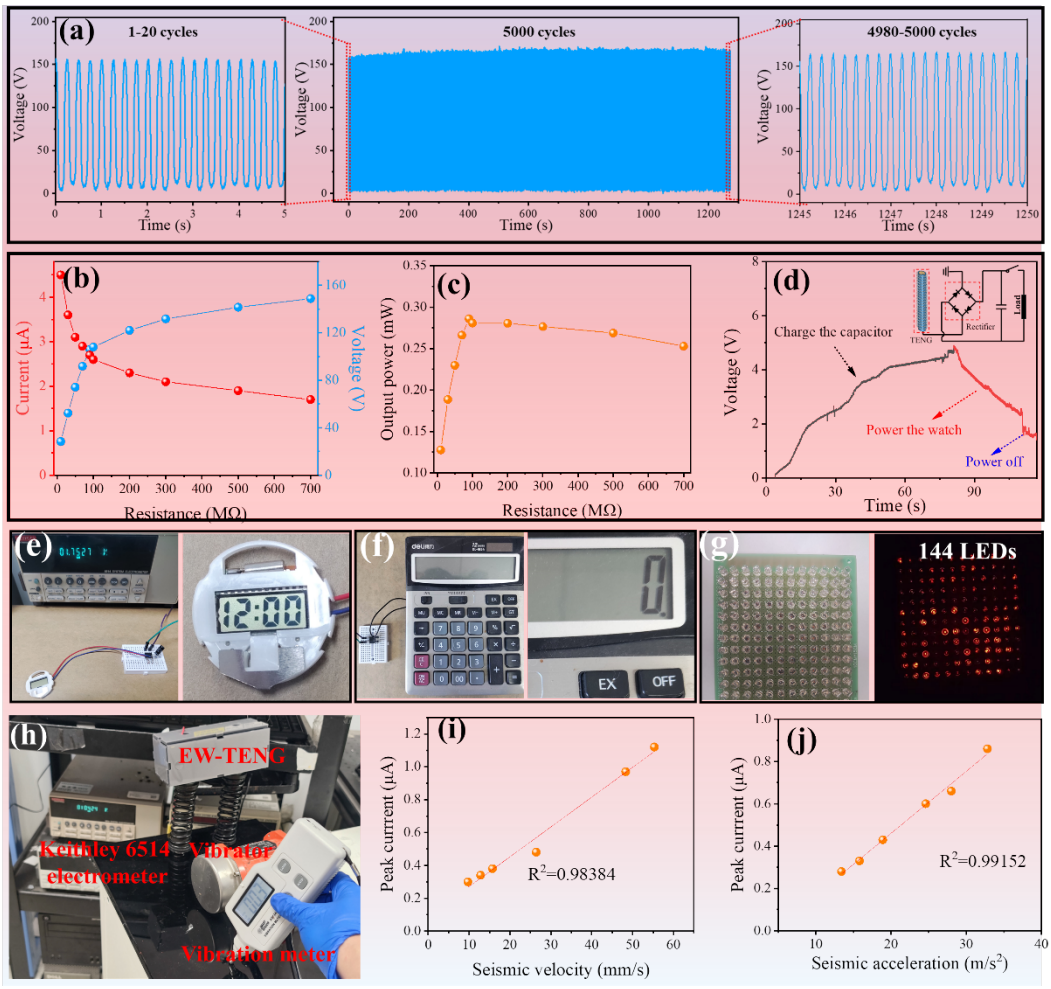

Fig. 5. Response of EW-TENG for 5000 cycles (a). Relation between current/voltage of EW-TENG and external resistance (b). Relationship between output power and varying load resistance (c). Charging and discharging curves of 33μF capacitor powered by EW-TENG and powering electronic watch at a frequency of 4 Hz (d). Digital images of EW-TENG powers electronic watch (e) and calculator (f). Digital image of EW-TENG illuminating 144 LEDs(g). Experimental setup for EW-TENG (h). Seismic velocity (i) and seismic (j) acceleration versus peak current plot.

The global Internet of Things (IoT) seismic network based on the EW-TENG could be constructed within the Earth's crust to provide earthquake warning by detecting longitudinal waves that propagate fast but are minor destructive. After earthquakes, the

EW-TENG array outputs data, and sent to the signal tower after measurements. These data are analyzed and compared to determine the magnitude and location of the earthquakes, and alert messages are issued to the area most likely to experience strong earthquakes. Upon receiving the alerts, people can take immediate action to avoid potential dangers (Fig. 6c). In order to emphasize the effectiveness of the EW-TENG for earthquake warning, the EW-TENG array is individually integrated inside globes filled with dirt and sand, as shown in Fig. 6a and Video S2, and the alarm system built based on the EW-TENG is shown in Fig. 6b. When the EW-TENG output is greater than a certain range, the electrical signal of the EW-TENG is recognized by MCU and sends to a Bluetooth command signal to activate the alarm (Video S3). It can remind people in the room to take necessary precautions during earthquakes. The workflow of the earthquake warning system is shown in Fig. 6c, further expanding the application of the EW-TENG in clean energy and advancing the development of earthquake warning technology. By varying the intensity and center of vibration (Fig. 6d and Fig. S5), different output voltages can be obtained. Subsequently, the performance of the device is validated in a more realistic simulated geological disaster scenario. As shown in Figure 4e, the device is positioned at different distances and orientations from the vibration source, enabling real-time monitoring by the EW-TENG system. According to the results of monitoring data, the possibility of the EW-TENG system monitoring response to earthquake is analyzed. The electrical signal diminishes as the distance from the vibration source increases, allowing for the determination of the vibration location through signal analysis. In addition, Fig. S6 demonstrates the performance of the EW-TENG integrated into different body parts. Integrating multiple EW-TENG at different body parts to establish human body activity monitoring, including neck movement, elbow bend, finger bend, wrist movement, ankle movement, and knee bend. The EW-TENG can effectively monitors external pressure, corroborating the potential application prospects of the EW-TENG in detecting human body activities and joint movements.

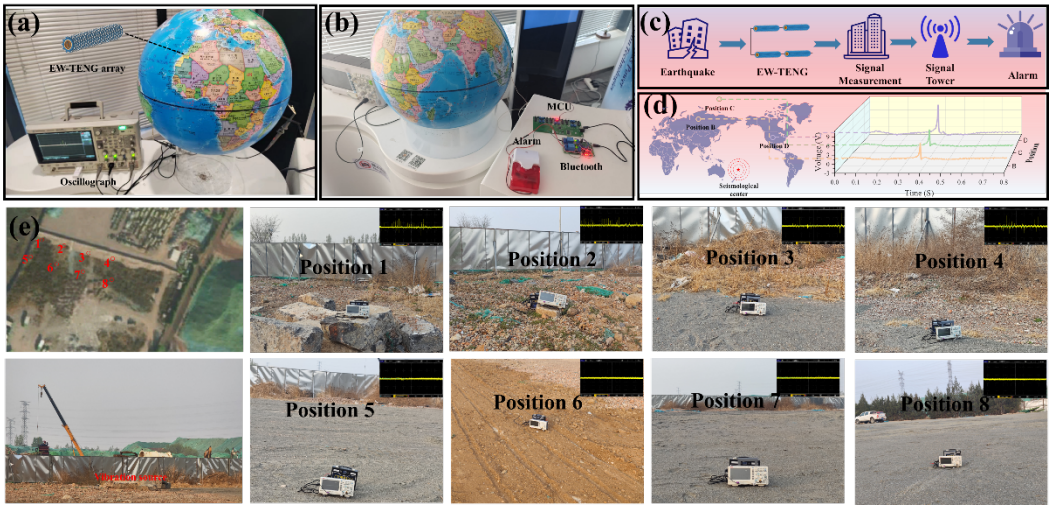

Fig. 6. Digital image showing the EW-TENG working as seismic wave detector for better earthquake warning (a, b). Workflow of the earthquake warning system (c). Real-time signal of the EW-TENG applied to monitor the vibration (d). Experimental setting and scene of outdoor test of earthquake system (e).

3 Conclusions

In summary, a self-powered earthquake warning sensor based on the EW-TENG is proposed for the detection of seismic P-waves. The EW-TENG comprises a hollow tubular copper electrodes and lotus-leaf inspired modified Ecoflex friction material. Benefiting from the friction material with the superhydrophobic coating that is constructed with nano SiO_2 on the Ecofelx surface with a complex surface texture, EW-TENG exhibits excellent superhydrophobicity, flame retardancy, and self-cleaning properties with output voltage of 142 V and current of 7.1 μA at the frequency of 5 Hz. In addition, at the optimal load of 90 MΩ, the peak power of the EW-TENG reaches 0.29 mW, and the peak power density reaches 15.4 mW/m², which is capable of powering electronic watch and calculator, or illuminating 144 LEDs. In addition, there is a strong linear correlation ($R^2 > 0.98$) between peak current and vibration acceleration and vibration. Ultimately, the EW-TENG has been shown to apply nearly every aspect of the earthquake warning, making it a promising future

detection of seismic P-waves, as well as expecting to build a global IoT earthquake warning network given their low cost, self-powering, high durability, and stability.

4 Experimental methods

Fabrication of the pre-treat Ecoflex

Ecoflex film was prepared by mixing commercial base (part A) and curing agent (part B) at a weight ratio of 1:1, and the mixture was poured into a prefabricated template and cured at room temperature for 4 h. Modified Ecoflex film was prepared in three steps. First, the abovementioned method was adopted to prepare the Ecoflex. Second, a PLS6.75 Laser system (4006-715-565) was performed to pre-treat the Ecoflex surface along a grid-like line with a line spacing of 244 μm. Finally, the abovementioned mixture was spin-coated onto the pre-treated Ecoflex film on a KW-A spin-coater at 3000 rpm. After curding at room temperature for 10 min, a large amount of nano SiO2 were uniformly coated on the film and cured at 120°C for 12 h.

Fabrication of system based on EW-TENG

The system mainly consists of a collision-based power generator and a receiver. The collision-based power generator can be made from a single material or a composite of several materials. The receiver can be composed of one or more types of semiconductors, conductors, or composite materials that are resistant to high temperatures and have excellent mechanical properties. The EW-TENG comprises a hollow electrode and a friction layer. A tubular structure with braided copper wire was selected as an electrode of EW-TENG, and the as-prepared modified Ecoflex film was selected as a friction layer. The modified Ecoflex film was adhered to the hollow electrode.

Characterization

The surface morphologies of modified Ecoflex film were observed by a NanoSEM 450 scanning electron microscopy. Water contact angles were measured by a contact angle meter (SDC-350) with 2 μL water droplets. The output current and voltage of EW-TENG

were measured by an electrometer (Keithley 6514). An attached vibrator (ZK-0.15S) was used to apply different vibration intensities to the EW-TENG. The vibration velocity/acceleration were tested by vibration meter (AS68A).

References

[1] A. Bhardwaj, S. Singh, L. Sam, et al. a review on remotely sensed land surface temperature anomaly as an earthquake precursor. Int J Appl Earth Obs Geoinformation. 2017, 63: 158–66.

[2] A.I. Chung. the development of earthquake early warning methods. Nat Rev Earth Environ. 2020, 1(7): 331–331.

[3] C.D. De Groot-Hedlin. seismic t-wave observations at dense seismic networks. Seismol Res Lett. 2020, 91(6): 3444–53.

[4] T.C. Lewis. artificial earthquakes. Nature. 1885, 32(822): 295–295.

[5] S. Tsuboi, M. Saito, and M. Kikuchi. real-time earthquake warning by using broadband p waveform. Geophys Res Lett [Internet]. 2002 [cited 2023], 29(24). Available from: https://agupubs.onlinelibrary.wiley.com/doi/10.1029/2002GL016101

[6] R.A. Sugondo and C. Machbub. p-wave detection using deep learning in time and frequency domain for imbalanced dataset. Heliyon. 2021, 7(12): e08605.

[7] Z. Yang, L. Wang, J. Qiao, et al. application and verification of a multivariate real-time early warning method for rainfall-induced landslides: implication for evolution of landslide-generated debris flows. Landslides. 2020, 17(10): 2409–19.

[8] Y. Yu, Q. Gao, X. Zhang, et al. contact-sliding-separation mode triboelectric nanogenerator. Energy Environ Sci. 2023, 16(9): 3932–41.

[9] Y. Li, X. Liu, Z. Ren, et al. marine biomaterial-based triboelectric nanogenerators: insights and applications. Nano Energy. 2024, 119: 109046.

[10] J. Wen, X. Pan, H. Fu, et al. advanced designs for electrochemically storing energy

from triboelectric nanogenerators. Matter. 2023, 6(7): 2153–81.

[11] X. Liu, Y. Liu, F. Liu, et al. high-performing honeycomb-structured triboelectric nanogenerator enhanced by triple electrodes for utilizing wind power. Nano Energy. 2023, 118: 108961.

[12] C. Xu, J. Yu, Z. Huo, et al. pursuing the tribovoltaic effect for direct-current triboelectric nanogenerators. Energy Environ Sci. 2023, 16(3): 983–1006.

[13] J. Luo, Z. Wang, L. Xu, et al. flexible and durable wood-based triboelectric nanogenerators for self-powered sensing in athletic big data analytics. Nat Commun. 2019, 10(1): 5147.

[14] L. Liu, M. Wu, W. Zhao, et al. progress of triboelectric nanogenerators with environmental adaptivity. Adv Funct Mater. 2023, : 2308353.

[15] H. Li, S. Lv, B. Zhang, et al. high power and low crest factor of direct-current triboelectric nanogenerator for self-powered optical computing system. Energy Environ Sci. 2023, 16(10): 4641–9.

[16] T. Cheng, J. Shao, and Z.L. Wang. triboelectric nanogenerators. Nat Rev Methods Primer. 2023, 3(1): 39.

[17] J. Yang, J. Chen, Y. Liu, et al. triboelectrification-based organic film nanogenerator for acoustic energy harvesting and self-powered active acoustic sensing. ACS Nano. 2014, 8(3): 2649–57.

[18] C.-H. Chen, P.-W. Lee, Y.-H. Tsao, et al. utilization of self-powered electrochemical systems: metallic nanoparticle synthesis and lactate detection. Nano Energy. 2017, 42: 241–8.

[19] Y. Hou, X. Dong, D. Li, et al. self-powered underwater force sensor based on a t-shaped triboelectric nanogenerator for simultaneous detection of normal and tangential forces. Adv Funct Mater. 2023, : 2305719.

[20] F. Liu, Y. Feng, Y. Qi, et al. self-powered wireless body area network for multi-joint movements monitoring based on contact-separation direct current triboelectric

nanogenerators. InfoMat. 2023, 5(8): e12428.

[21] S. Liu, S. Liu, Q. Wang, et al. improving surface performance of silicone rubber for composite insulators by multifunctional nano-coating. Chem Eng J. 2023, 451: 138679.

[22] S. Pan, R. Guo, J.J. Richardson, et al. ricocheting droplets moving on super-repellent surfaces. Adv Sci. 2019, 6(21): 1901846.

[23] P. Wang, C. Li, and D. Zhang. recent advances in chemical durability and mechanical stability of superhydrophobic materials: multi-strategy design and strengthening. J Mater Sci Technol. 2022, 129: 40–69.

[24] F. Li, X. Yue, L. Cheng, et al. hydrophobicity-aerophilicity effect boosting efficient co2 photoreduction in graphitic carbon nitride modified with fluorine-containing groups. Chem Eng J. 2023, 452: 139463.

[25] R. Nishimura, K. Hyodo, H. Sawaguchi, et al. fractal surfaces of molecular crystals mimicking lotus leaf with phototunable double roughness structures. J Am Chem Soc. 2016, 138(32): 10299–303.

[26] R.D. Mukhopadhyay, B. Vedhanarayanan, and A. Ajayaghosh. creation of “rose petal” and “lotus leaf” effects on alumina by surface functionalization and metal-ion coordination. Angew Chem Int Ed. 2017, 56(50): 16018–22.

[27] O. Tricinci, F. Pignatelli, and V. Mattoli. 3d micropatterned functional surface inspired by salvinia molesta via direct laser lithography for air retention and drag reduction. Adv Funct Mater. 2023, 33(39): 2206946.

[28] A.D. Lantada, S. Hengsbach, and K. Bade. lotus-on-chip: computer-aided design and 3d direct laser writing of bioinspired surfaces for controlling the wettability of materials and devices. Bioinspir Biomim. 2017, 12(6): 066004.

[29] X. Cao, M. Zhang, J. Huang, et al. inductor-free wireless energy delivery via maxwell’s displacement current from an electrodeless triboelectric nanogenerator. Adv Mater. 2018, 30(6): 1704077.

[30] J. Shao, M. Willatzen, T. Jiang, et al. quantifying the power output and structural figure-of-merits of triboelectric nanogenerators in a charging system starting from the maxwell's displacement current. Nano Energy. 2019, 59: 380–9.

[31] S. Zhang, M. Bick, X. Xiao, et al. leveraging triboelectric nanogenerators for bioengineering. Matter. 2021, 4(3): 845–87.

[32] Q. Zeng, A. Chen, X. Zhang, et al. a dual-functional triboelectric nanogenerator based on the comprehensive integration and synergetic utilization of triboelectrification, electrostatic induction, and electrostatic discharge to achieve alternating current/direct current convertible outputs. Adv Mater. 2023, 35(7): 2208139.

[33] W. Zhong, B. Xu, and Y. Gao. engraved pattern spacer triboelectric nanogenerators for mechanical energy harvesting. Nano Energy. 2022, 92: 106782.

[34] K. Ghosh, C. Iffelsberger, M. Konečný, et al. nanoarchitectonics of triboelectric nanogenerator for conversion of abundant mechanical energy to green hydrogen. Adv Energy Mater. n/a(n/a): 2203476.

[35] H. Wang, Z. Rao, Y. Liu, et al. a highly stretchable triboelectric nanogenerator with both stretch-insensitive sensing and stretch-sensitive sensing. Nano Energy. 2023, 107: 108170.

Acknowledgments

International and domestic patents have been filed to protect the reported inventions.